

# High-voltage lithium cathode materials

Hiroo Kawai <sup>a</sup>, Mikito Nagata <sup>b</sup>, Hisashi Tukamoto <sup>b</sup>, Anthony R. West <sup>a,\*</sup>

<sup>a</sup> Department of Chemistry, University of Aberdeen, Meston Walk, Aberdeen AB24 3UE, Scotland, UK

<sup>b</sup> Corporate R&D Center, Japan Storage Battery, Nishinosho, Kisshoin, Minami-ku, Kyoto 601, Japan

## Abstract

Single cell lithium battery systems can operate over 4.5 V vs. Li/Li<sup>+</sup> on the basis of reversible extraction of lithium from several cathodes based on complex spinel oxides Li<sub>2</sub>MM'<sub>3</sub>O<sub>8</sub> and LiMM'O<sub>4</sub>: MM'<sub>3</sub>=CrMn<sub>3</sub>, FeMn<sub>3</sub>, CoMn<sub>3</sub>, NiMn<sub>3</sub>, CuMn<sub>3</sub>; MM'=CrMn, CoMn, NiV. Except for LiNiVO<sub>4</sub>, Li<sup>+</sup> fully occupies tetrahedral sites and can, therefore, move through the well-known tetrahedral site-empty octahedral site pathway; Mn occupies octahedral sites, and exhibits mixed-valence states, so that fast electronic transport is expected to occur between neighboring Mn<sup>3+</sup>/Mn<sup>4+</sup>. In all cases, the electrochemical process over 4.5 V is attributable to the redox couples of M situated in octahedral sites: Cr<sup>3+/4+</sup>, Fe<sup>3+/4+</sup>, Co<sup>3+/4+</sup>, Ni<sup>2+/4+</sup>, Cu<sup>2+/3+</sup>. Of a potentially large family of spinel-based cathodes in the systems Li–M–M'–O, the largest capacity over 4.5 V achievable so far occurs when tetrahedral sites are fully occupied by lithium which is reversibly extracted by means of the redox couples of M located in octahedral sites. For example, a cell with LiCoMnO<sub>4</sub> exhibits a discharge capacity of ca. 95 mA h g<sup>-1</sup> at a plateau centered on 5.0 V and, therefore, has superior energy density and operating voltage to LiMn<sub>2</sub>O<sub>4</sub>, the favored cathode in next-generation lithium batteries. © 1999 Elsevier Science S.A. All rights reserved.

**Keywords:** Lithium; Cathode; Battery

## 1. Introduction

Lithium rechargeable batteries offer the highest energy density of all rechargeable battery systems [1] and give various applications ranging in size from portable electronic devices to zero emission vehicles (ZEV) [1,2]. The requirements for advanced lithium rechargeable batteries include high energy and power density, reversibility and cyclability, safety, limited environmental impact and low cost [1,2]. Improved performance is achieved with new or improved anodes, electrolytes or cathodes [1–4].

LiCoO<sub>2</sub> [5] was the first cathode to be used in commercial lithium ion rechargeable cells [6], and operates at ca. 3.7 V vs. Li/Li<sup>+</sup>. A recent approach is to replace expensive and toxic LiCoO<sub>2</sub> by the 3.8 V cathode LiMn<sub>2</sub>O<sub>4</sub> [7–9], in state-of-the-art cells [10]. These cells can successfully substitute for conventional nickel–cadmium systems in portable electronic devices [11], but larger scale batteries for ZEV require further improvement in energy density by either increasing capacity or raising operating voltage. Cells with LiMnO<sub>2</sub> [12,13] and Li<sub>1.5</sub>Na<sub>0.5</sub>MnO<sub>2.85</sub>I<sub>0.12</sub> [14] as cathodes exhibited larger capacity, but the former

needs improved cycling stability and the latter would require higher working voltage. Improved electrolytes [15,16] have recently made it possible to explore the potential range to ca. 5 V. Cells with high operating voltage have been reported with cathodes based on spinel structure oxides, including 4.7 V for LiNi<sub>x</sub>Mn<sub>2-x</sub>O<sub>4</sub> [17,18], 4.8 V for LiNiVO<sub>4</sub> [19] and LiCr<sub>x</sub>Mn<sub>2-x</sub>O<sub>4</sub> [20] and 4.9 V for LiCu<sub>x</sub>Mn<sub>2-x</sub>O<sub>4</sub> [21,22]. We recently reported the first single cell lithium battery systems to operate over 5 V, by the incorporation of novel spinel cathodes, Li<sub>2</sub>CoMn<sub>3</sub>O<sub>8</sub> [23] and LiCoMnO<sub>4</sub> [24]: the latter showed superior energy density and operating voltage to LiMn<sub>2</sub>O<sub>4</sub> [24]. Subsequently, we found the much cheaper and less toxic spinel cathode Li<sub>2</sub>FeMn<sub>3</sub>O<sub>8</sub> to operate at a discharge plateau ranging from 5.0 V to 4.8 V [25]. Here we review and discuss structural, compositional and electrochemical aspects of lithium cathode materials that operate over 4.5 V.

## 2. Synthesis and structure

The ideal spinel structure consists of a cubic close-packed array of anions, with one-eighth of the tetrahedral

\* Corresponding author

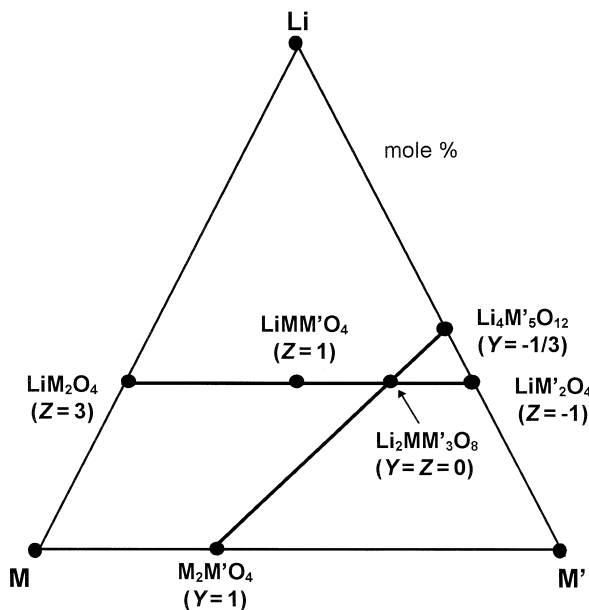


Fig. 1. Possible formation of spinel solid solutions  $\text{Li}_{2-2Y}\text{M}_{1+3Y}\text{M}'_{3-Y}\text{O}_8$  and  $\text{Li}_2\text{M}_{1+Z}\text{M}'_{3-Z}\text{O}_8$  in the systems Li–M–M'–O. Oxygen contents are not specified.

and one-half of the octahedral interstices occupied by cations, having the general formula  $\text{A}[\text{B}_2]\text{X}_4$ , where A is a tetrahedrally surrounded cation, B an octahedrally surrounded one, and X an anion. Possible lithium cathode materials that operate over 4.5 V are in a potentially large family of spinel-structure oxides in the systems Li–M–M'–O which includes two series of possible solid solutions of general formulae  $\text{Li}_{2-2Y}\text{M}_{1+3Y}\text{M}'_{3-Y}\text{O}_8$  between  $\text{Li}_4\text{M}'_5\text{O}_{12}$  ( $Y = -1/3$ ) and  $\text{M}_2\text{M}'\text{O}_4$  ( $Y = 1$ ) and  $\text{Li}_2\text{M}_{1+Z}\text{M}'_{3-Z}\text{O}_8$  between  $\text{LiM}'_2\text{O}_4$  ( $Z = -1$ ) and  $\text{LiM}_2\text{O}_4$  ( $Z = 3$ ), Fig. 1 [24]. Materials identified so far are  $\text{Li}_2\text{MM}'_3\text{O}_8$  ( $Y = Z = 0$ ) and  $\text{LiMM}'\text{O}_4$  ( $Z = 1$ ):  $\text{MM}'_3 = \text{CrMn}_3, \text{FeMn}_3, \text{CoMn}_3, \text{NiMn}_3, \text{CuMn}_3$ ;  $\text{MM}' = \text{CrMn}, \text{CoMn}, \text{NiV}$ , Table 1. Several of these exhibit cation order on the octahedral sites, i.e., 1:3 order for many  $\text{Li}_2\text{MM}'_3\text{O}_8$  spinels [26–28] and 1:1 order for several  $\text{LiMM}'\text{O}_4$  spinels [26,29,30] and, therefore, they are regarded as separate

phases rather than as solid solutions based on binary spinels such as  $\text{LiMn}_2\text{O}_4$  or  $\text{Co}_2\text{MnO}_4$ . In the following text, M represents Cr, Fe, Co, Ni and Cu.

Oxygen loss associated with the reduction of Mn is likely to occur at high temperatures for many spinels containing  $\text{Mn}^{4+}$ , and was in fact observed in air above  $650^\circ\text{C}$  for  $\text{Li}_2\text{CoMn}_3\text{O}_8$  [23]. Conventional ceramic synthesis under oxidizing conditions has been used as a general technique to prepare spinel phases listed in Table 1 [25,26]. The following compositions formed spinel phases in air, subject to either post-reaction anneal or slow-cooling to optimize their oxygen contents:  $\text{Li}_2\text{CrMn}_3\text{O}_8$  [20],  $\text{LiCrMnO}_4$  [20,31],  $\text{Li}_2\text{CoMn}_3\text{O}_8$  [23] and  $\text{LiCoMnO}_4$  [24,31]. Conventional ceramic synthesis of  $\text{LiNiVO}_4$  [19],  $\text{Li}_2\text{NiMn}_3\text{O}_8$  [17,32] and  $\text{Li}_2\text{CuMn}_3\text{O}_8$  [21,22] gave mainly a single phase but with small amounts of impurities, but by low-temperature synthesis, phase-pure  $\text{LiNiVO}_4$  [33,34] and  $\text{Li}_2\text{NiMn}_3\text{O}_8$  [17,18,32] were prepared; the phase purity of  $\text{Li}_2\text{CuMn}_3\text{O}_8$  was improved by sol-gel synthesis, but small amounts of impurities detectable from powder neutron diffraction data remained [22].

Powder XRD patterns of all spinels listed in Table 1 were indexed in the cubic space group,  $Fd\bar{3}m$  with  $8.05 < a/\text{\AA} < 8.26$ . Rietveld refinement was carried out using powder XRD data for  $\text{Li}_2\text{CrMn}_3\text{O}_8$  [35],  $\text{LiCrMnO}_4$  [35,36],  $\text{Li}_2\text{FeMn}_3\text{O}_8$  [25],  $\text{Li}_2\text{CoMn}_3\text{O}_8$  [23],  $\text{LiCoMnO}_4$  [24] and  $\text{LiNiVO}_4$  [37] and combined powder XRD and neutron diffraction data for  $\text{Li}_2\text{CuMn}_3\text{O}_8$  [22]; cation distributions were estimated approximately by comparing the observed XRD patterns to several theoretical ones [26] or by observing the intensity of the (220) peak [18] for  $\text{Li}_2\text{NiMn}_3\text{O}_8$ .  $\text{LiNiVO}_4$  refined essentially as an inverse spinel,  $\text{V}[\text{LiNi}]_4\text{O}_4$ : V fully occupied tetrahedral  $8a$  sites; Li and Ni in 1:1 ratio were disordered over octahedral  $16d$  sites, Table 1. All others refined to normal spinels,  $\text{Li}[\text{M}_{0.5}\text{Mn}_{1.5}]\text{O}_4$  or  $\text{Li}[\text{MMn}]\text{O}_4$  with Li in tetrahedral  $8a$  sites and M, Mn in octahedral  $16d$  sites with ratio 1:3 or 1:1, Table 1.  $\text{Li}_2\text{CuMn}_3\text{O}_8$  was proposed to be  $\text{Li}[\text{Cu}_{0.5}\text{Mn}_{1.5}]\text{O}_4$  [26], but was more recently shown to contain small amounts of impurities together with a main

Table 1

Structural data for high-voltage lithium cathode materials,  $\text{Li}_2\text{MM}'_3\text{O}_8$  and  $\text{LiMM}'\text{O}_4$  based on spinel-structure oxides

Composition	Symmetry (Space group)	Lattice parameter <sup>a</sup> $a/\text{\AA}$	Cation distributions <sup>b</sup>	Charge distributions	References
$\text{Li}_2\text{CrMn}_3\text{O}_8$	Cubic ( $Fd\bar{3}m$ )	8.208	$\text{Li}[\text{Cr}_{0.5}\text{Mn}_{1.5}]$	$\text{Li}^+\text{Cr}^{3+}\text{Mn}^{3+}\text{Mn}^{4+}\text{O}_8$	[35]
$\text{LiCrMnO}_4$	Cubic ( $Fd\bar{3}m$ )	8.189	$\text{Li}[\text{CrMn}]$	$\text{Li}^+\text{Cr}^{3+}\text{Mn}^{4+}\text{O}_4$	[26,31,35,36]
$\text{Li}_2\text{FeMn}_3\text{O}_8$	Cubic ( $Fd\bar{3}m$ )	8.251	$\text{Li}[\text{Fe}_{0.5}\text{Mn}_{1.5}]$	$\text{Li}_2^+\text{Fe}^{3+}\text{Mn}^{3+}\text{Mn}^{4+}\text{O}_8$	[25]
$\text{Li}_2\text{CoMn}_3\text{O}_8$	Cubic ( $Fd\bar{3}m$ )	8.132	$\text{Li}[\text{Co}_{0.5}\text{Mn}_{1.5}]$	$\text{Li}_2^+\text{Co}^{3+}\text{Mn}^{3+}\text{Mn}^{4+}\text{O}_8$	[23,26,38]
$\text{LiCoMnO}_4$	Cubic ( $Fd\bar{3}m$ )	8.052	$\text{Li}[\text{CoMn}]$	$\text{Li}^+\text{Co}^{3+}\text{Mn}^{4+}\text{O}_4$	[24,26,31]
$\text{LiNiVO}_4$	Cubic ( $Fd\bar{3}m$ )	8.222	$\text{V}[\text{LiNi}]$	$\text{Li}^+\text{Ni}^{2+}\text{V}^{5+}\text{O}_4$	[26,37,39]
$\text{Li}_2\text{NiMn}_3\text{O}_8$	Cubic ( $Fd\bar{3}m$ )	8.172	$\text{Li}[\text{Ni}_{0.5}\text{Mn}_{1.5}]$	$\text{Li}_2^+\text{Ni}^{2+}\text{Mn}^{3+}\text{O}_8$	[18,26,32,40]
$\text{Li}_2\text{CuMn}_3\text{O}_8$	Cubic ( $Fd\bar{3}m$ )	8.199	$\text{Li}_{0.9}\text{Cu}_{0.1}[\text{Li}_{0.11}\text{Cu}_{0.22}\text{Mn}_{1.67}]$	$\text{Li}_{2.02}^+\text{Cu}_{0.64}^{2+}\text{Mn}_{0.66}^{3+}\text{Mn}_{2.68}^{4+}\text{O}_8$	[22,26]

<sup>a</sup>For each composition, one lattice parameter is chosen arbitrarily from the reference list.

<sup>b</sup>In  $\text{A}[\text{B}_2]\text{O}_4$ , A denotes tetrahedral  $8a$  sites, and B octahedral  $16d$  sites.

spinel phase,  $\text{Li}_{2.02}\text{Cu}_{0.64}\text{Mn}_{3.34}\text{O}_8$  which refined to  $\text{Li}_{0.9}\text{Cu}_{0.1}[\text{Li}_{0.11}\text{Cu}_{0.22}\text{Mn}_{1.67}]\text{O}_4$  [22], Table 1. M and Mn have very similar atomic scattering factors, and thus powder XRD data offer little information about possible 1:3 or 1:1 ordering between M and Mn in octahedral sites: further structural study on possible octahedral cation ordering is needed.

Various solid state techniques were used to estimate cation charges, Table 1. For  $\text{Li}_2\text{CrMn}_3\text{O}_8$  and  $\text{LiCrMnO}_4$ , the valence states of Cr and Mn were determined from electron energy loss spectroscopy (EELS), consistent with the charge distributions  $\text{Li}_2^+\text{Cr}^{3+}\text{Mn}^{3+}\text{Mn}_2^{4+}\text{O}_8$  [35] and  $\text{Li}^+\text{Cr}^{3+}\text{Mn}^{4+}\text{O}_4$  [31,35].  $\text{Li}_2\text{FeMn}_3\text{O}_8$  was found to be  $\text{Li}_2^+\text{Fe}^{3+}\text{Mn}^{3+}\text{Mn}_2^{4+}\text{O}_8$  from combined  $^{57}\text{Fe}$  Mössbauer and magnetic susceptibility data [25]. For  $\text{Li}_2\text{CoMn}_3\text{O}_8$ , the valence states of Co and Mn were determined from X-ray absorption near edge structure (XANES), consistent with the formula,  $\text{Li}_2^+\text{Co}^{3+}\text{Mn}^{3+}\text{Mn}_2^{4+}\text{O}_8$  [38]. For  $\text{LiCoMnO}_4$ , EELS indicated the formula,  $\text{Li}^+\text{Co}^{3+}\text{Mn}^{4+}\text{O}_4$  [31]. For  $\text{LiNiVO}_4$ , the charge distribution was estimated to be  $\text{Li}^+\text{Ni}^{2+}\text{V}^{5+}\text{O}_4$  on the basis of magnetic susceptibility data [39]. For  $\text{Li}_2\text{NiMn}_3\text{O}_8$ , X-ray photoelectron spectroscopy (XPS) [32] and ultraviolet photoelectron spectroscopy (UPS) [40] indicated the presence of  $\text{Ni}^{2+}$ , and assuming oxygen stoichiometry, the valence distribution,  $\text{Li}_2^+\text{Ni}^{2+}\text{Mn}_3^{4+}\text{O}_8$ . For  $\text{Li}_2\text{CuMn}_3\text{O}_8$ , XANES spectra of Cu and Mn edges indicated the charge distribution,  $\text{Li}_{2.02}^+\text{Cu}_{0.64}^{2+}\text{Mn}_{0.66}^{3+}\text{Mn}_{2.68}^{4+}\text{O}_8$  [22].

### 3. Electrochemical properties

Electrochemical extraction of lithium from many of the Mn-based spinels takes place reversibly, initially at a plateau centered on ca. 4.0 V along with the oxidation of  $\text{Mn}^{3+}$  to  $\text{Mn}^{4+}$  provided that  $\text{Mn}^{3+}$  is present, then at a second plateau over 4.5 V along with oxidation of M situated in octahedral sites. The potential profiles of the cells:  $\text{Li}/\text{Li}_2\text{CoMn}_3\text{O}_8$  [23] and  $\text{Li}/\text{LiCoMnO}_4$  [24] are shown in Figs. 2 and 3.

The average discharge voltage at the plateau over 4.5 V and its associated redox couple are listed in Table 2. The  $\text{Co}^{3+/4+}$  couple in  $\text{Li}_2\text{CoMn}_3\text{O}_8$  [23,38] and  $\text{LiCoMnO}_4$  [24] operated at discharge plateaux centered on 5.1 V, Fig. 2, and 5.0 V, Fig. 3, respectively. The  $\text{Cu}^{2+/3+}$  couple in  $\text{Li}_2\text{CuMn}_3\text{O}_8$  [22] and the  $\text{Fe}^{3+/4+}$  couple in  $\text{Li}_2\text{FeMn}_3\text{O}_8$  [25] both operated at a discharge plateau commencing at 5.0 V and centered on 4.9 V. The  $\text{Cr}^{3+/4+}$  couple in  $\text{Li}_2\text{CrMn}_3\text{O}_8$  and  $\text{LiCrMnO}_4$  operated at a discharge plateau centered on 4.8 V [35]. Redox couple(s) of Ni in  $\text{LiNiVO}_4$  operated at mid-discharge voltage of 4.8 V [19]. The  $\text{Ni}^{2+/4+}$  couple in  $\text{Li}_2\text{NiMn}_3\text{O}_8$  operated at a discharge plateau centered on 4.7 V [17,18,40,41].

The spinel  $\text{LiCoMnO}_4$  [24] and the layered rock-salt  $\text{LiCoO}_2$  [5] operate as a lithium cathode by means of the

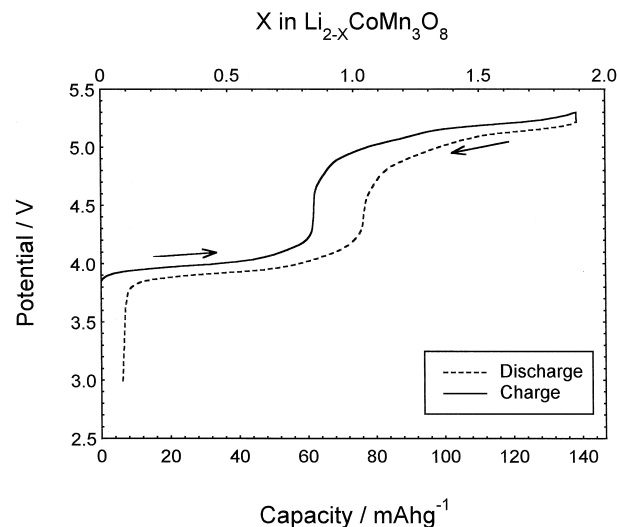


Fig. 2. Initial charge–discharge profile for a cell,  $\text{Li}/\text{LiPF}_6$ , propylene carbonate/ $\text{Li}_2\text{CoMn}_3\text{O}_8$ , Ref. [23].

$\text{Co}^{3+/4+}$  couple which, in both cases, occupies octahedral interstices surrounded by cubic close-packed oxygens. Cells with  $\text{LiCoMnO}_4$ , however, exhibit much higher mid-discharge voltage of 5.0 V, Fig. 3, compared with 3.7 V [42] for those with  $\text{LiCoO}_2$ . The voltage increase in  $\text{LiCoMnO}_4$  must originate in either decrease in site energy of  $\text{Li}^+$  which occupies octahedral interstices in  $\text{LiCoO}_2$ , but distributes over tetrahedral interstices in  $\text{LiCoMnO}_4$  or change in electronic structure, induced by the octahedra containing Mn which are absent in  $\text{LiCoO}_2$ , but coexist with the octahedra containing Co in  $\text{LiCoMnO}_4$ , restricting the interconnection between the octahedra containing Co. It should be noted that all high-voltage cathode materials except for  $\text{LiNiVO}_4$  have normal spinel structure with the tetrahedral interstices fully occupied by Li and the octahedral interstices containing a mixture of M and Mn, Table 1.

Recently, cell voltage was reported to increase by the partial replacement of Co with Al in  $\text{LiCoO}_2$  [43]. This voltage rise was ascribed through first-principles pseudopotential calculations to substantial charge transfer to oxygen, instead of Co, during the electrochemical processes, since the fixed 3+ valence of Al can force electron exchange to occur with oxygen [43,44]. The lithium intercalation voltage was estimated to be 5.3 V for a hypothetical solid oxide with cubic close-packing [44]. If this interpretation is correct, cell voltage must increase by the partial or complete substitution of non-transition metals for transition metals in any lithium cathode material based on transition-metal oxides including the high-voltage cathode materials discussed here: substitution of Al for Co in  $\text{Li}_2\text{CoMn}_3\text{O}_8$ , for instance, should lead to average discharge voltage above 5.1 V. However, evidence of substantial charge transfer to oxygen was not found in  $\text{Li}(\text{Co,Al})\text{O}_2$  [43] and, therefore, the voltage rise observed

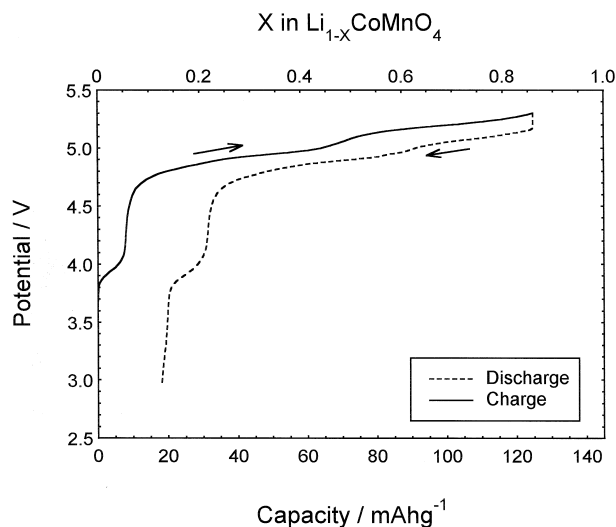


Fig. 3. Initial charge–discharge profile for a cell, Li/LiPF<sub>6</sub>, propylene carbonate/LiCoMnO<sub>4</sub>, Ref. [24].

may arise from the change in cation distributions over octahedral interstices, including Li sites, after substitution of Al, followed by possible structural deformations: detailed structural study is needed to clarify the origin of the voltage rise.

In the ideal normal spinel structure A[B<sub>2</sub>]X<sub>4</sub>, space group *Fd3m*, each 8*a* tetrahedron occupied by A-cations shares common faces with four neighboring empty 16*c* octahedra. A-cations can, therefore, move three-dimensionally through the possible diffusion pathway, 8*a* → 16*c* → 8*a* → 16*c* → . All high-voltage cathodes except LiNiVO<sub>4</sub> are normal spinels with all Li situated in tetrahedral 8*a* sites, Table 1, and thus long range Li<sup>+</sup> migration can occur through the above pathway. Partial occupancy of tetrahedral sites by immobile cations may act as channel blocking agents, leading to an increase in activation energy for Li<sup>+</sup> conduction [28]. LiNiVO<sub>4</sub> has an essentially inverse spinel structure, Table 1 [37]: if all the Li were located in octahedral 16*d* sites, no Li<sup>+</sup> conduction would be expected through the tetrahedral site-empty octahedral site pathway. Small, but considerable amounts of Li in LiNiVO<sub>4</sub> were, however, reversibly extracted and inserted in Li/LiNiVO<sub>4</sub> electrochemical cells, Table 2 [19,33,37].

During reversible extraction of lithium from the cathodes, electron (hole) migration accompanies Li<sup>+</sup> migration to maintain charge neutrality. High electronic conductivity in oxides has been most frequently observed in mixed valency semiconductors [45] which require cations of the same element, but with oxidation states differing by unity, situated in crystallographically similar sites. For spinels such as Mn<sub>3</sub>O<sub>4</sub> [46,47], NiMn<sub>2</sub>O<sub>4</sub> [46] and LiMn<sub>2</sub>O<sub>4</sub> [48], fast electronic transport is attained by thermally activated, small polaron hopping between Mn<sup>3+</sup>/Mn<sup>4+</sup> in adjacent octahedral sites. Li<sub>2</sub>CoMn<sub>3</sub>O<sub>8</sub> exhibits high electronic conductivity [23], ascribable to the presence of neighboring Mn<sup>3+</sup>/Mn<sup>4+</sup> interconnected over three quarters of the

octahedral sites, Table 1. Li<sub>2</sub>NiGe<sub>3</sub>O<sub>8</sub> is a normal spinel with 1:3 order of Ni<sup>2+</sup> and Ge<sup>4+</sup> in octahedral sites: octahedra containing Ge<sup>4+</sup> are interconnected, but Ni<sup>2+</sup> octahedra are completely isolated by these Ge<sup>4+</sup> octahedra, to prevent any interconnection between Ni<sup>2+</sup> octahedra [28]. Li<sub>2</sub>NiGe<sub>3</sub>O<sub>8</sub> was found to be electrochemically inactive as a lithium cathode since although Li<sup>+</sup> migration and oxidation of Ni<sup>2+</sup> are certainly feasible, there was no measurable electronic conduction, attributable to the absence of mixed-valence states for Ge [28].

The theoretical total capacities are defined as the capacities obtainable from the as-prepared, fully discharged compositions listed in Table 2 to the corresponding fully charged compositions. For the fully discharged composition Li<sub>2.02</sub>Cu<sub>0.64</sub>Mn<sub>3.34</sub>O<sub>8</sub>, the fully charged composition is limited to Li<sub>1.70</sub>Cu<sub>0.64</sub>Mn<sub>3.34</sub>O<sub>8</sub> which already achieved oxidation of Cu and Mn; for the other fully discharged compositions, the redox reactions allow reaching the fully charged compositions, MM'<sub>3</sub>O<sub>8</sub> or MM'<sub>4</sub>O<sub>4</sub>. The theoretical capacities at the plateaux centered on ca. 4.0 V correspond to the capacities obtainable by the oxidation to Mn<sup>4+</sup> of Mn<sup>3+</sup> present at the fully discharged compositions listed in Table 1, and these capacities subtracted from the corresponding theoretical total capacities leave the theoretical capacities at the plateaux over 4.5 V, associated with the redox reactions of M. It is seen from Table 2 that the observed discharge capacities at the plateaux centered on ca. 4.0 V agree well with the corresponding theoretical ones. LiCoMnO<sub>4</sub> [24] and Li<sub>2</sub>NiMn<sub>3</sub>O<sub>8</sub> [17] appear to contain small amounts of Mn<sup>3+</sup>, having a fully discharged state slightly different from respectively Li<sup>+</sup>Co<sup>3+</sup>Mn<sup>4+</sup>O<sub>4</sub> and Li<sub>2</sub>Ni<sup>2+</sup>Mn<sub>3</sub><sup>4+</sup>O<sub>8</sub> listed in Table 1, since there existed small capacities at the discharge plateaux centered on ca. 4.0 V, Table 2: Fig. 3 reveals slight evidences of the plateau centered on 3.9 V for the Li/LiCoMnO<sub>4</sub> cell. Discharge capacities obtained at the plateaux over 4.5 V are considerably smaller than expected, Table 2. Electrolyte oxidation occurs above ca. 5.0 V in currently available electrolytes [15,16] and, thus, the potential scan is at present limited to ca. 5.3 V, Table 2. Further improvement in electrolyte stability is required to measure electrochemical properties at higher potentials.

Although electrolyte oxidation does not allow us to fully evaluate cathode properties at high voltage, one of the largest capacities over 4.5 V would certainly be achievable by having tetrahedral interstices fully occupied by Li all of which is reversibly extracted by means of the redox couple of M situated in octahedral sites. Suitable compositions can be chosen from a potentially large family of spinel-structure oxides in the systems Li–M–M'–O, Fig. 1 [24]. The simplest models include: (1) Li[M<sub>0.5</sub><sup>2+</sup>M'<sub>1.5</sub><sup>4+</sup>]O<sub>4</sub> linked to the M<sup>2+/4+</sup> couple; (2) Li[M<sup>3+</sup>M'<sup>4+</sup>]O<sub>4</sub> linked to the M<sup>3+/4+</sup> couple; (3) Li[M<sup>2+</sup>M'<sup>5+</sup>]O<sub>4</sub> linked to either M<sup>2+/4+</sup> or M<sup>2+/3+</sup> couple. Three examples of the above are known: Li<sub>2</sub>Ni<sup>2+</sup>Mn<sub>3</sub><sup>4+</sup>O<sub>8</sub> (1), LiCr<sup>3+</sup>Mn<sup>4+</sup>O<sub>4</sub> (2) and LiCo<sup>3+</sup>Mn<sup>4+</sup>O<sub>4</sub> (2), and the corresponding

Table 2  
Electrochemical data for high-voltage lithium cathode materials,  $\text{Li}_2\text{MM}'_3\text{O}_8$  and  $\text{LiMM}'\text{O}_4$  based on spinel-structure oxides

Composition	Mid-discharge voltage at the plateau over 4.5 V/V	Redox couple <sup>b</sup> to operate at the plateau over 4.5 V	Theoretical capacity <sup>d</sup> at the plateau centered on 4.0 V/mA h g <sup>-1</sup>	Theoretical capacity <sup>d</sup> at the plateau over 4.5 V/mA h g <sup>-1</sup>	Observed capacity <sup>e</sup> at the plateau centered on 4.0 V/mA h g <sup>-1</sup>	Observed capacity <sup>e</sup> at the plateau over 4.5 V/mA h g <sup>-1</sup>	Potential range/V	References
$\text{Li}_2\text{CrMn}_3\text{O}_8$	4.8	$\text{Cr}^{3+/4+}$	75	75	70	55	3.4–5.4	[20,35]
$\text{LiCrMnO}_4$	4.8	$\text{Cr}^{3+/4+}$	0	151	0 <sup>f</sup>	75 <sup>f</sup>	3.4–5.4	[20,35]
$\text{Li}_2\text{FeMn}_3\text{O}_8$	4.9	$\text{Fe}^{3+/4+}$	74	74	75	50	3.0–5.3	[25]
$\text{Li}_2\text{CoMn}_3\text{O}_8$	5.1	$\text{Co}^{3+/4+}$	73	73	70	60	3.0–5.3	[23,38]
$\text{LiCoMnO}_4$	5.0	$\text{Co}^{3+/4+}$	0	145	10	95	3.0–5.3	[24]
$\text{LiNiVO}_4$	4.8	$\text{Ni}^{2+/3+/4+c}$	0	148	0	45	3.0–4.9	[19]
$\text{Li}_2\text{NiMn}_3\text{O}_8$	4.7	$\text{Ni}^{2+/4+}$	0	147	16	95	3.0–4.9	[17,40,41]
$\text{Li}_{2.02}\text{Cu}_{0.64}\text{Mn}_{3.34}\text{O}_8^a$	4.9	$\text{Cu}^{2+/3+}$	48	47	48	23	3.3–5.1	[22]

<sup>a</sup>Composition of the spinel component at the nominal composition  $\text{Li}_2\text{CuMn}_3\text{O}_8$ .

<sup>b</sup>All redox couples are located in octahedral sites.

<sup>c</sup>There remains three possibilities:  $\text{Ni}^{2+/3+}$ ,  $\text{Ni}^{3+/4+}$ , and  $\text{Ni}^{2+/4+}$ .

<sup>d</sup>For the calculation procedure, see text.

<sup>e</sup>Estimated from initial discharge profiles.

<sup>f</sup>An inclined single plateau ranging between 3.8–4.8 V was observed.

charge–discharge profiles of cells with  $\text{Li}_2\text{NiMn}_3\text{O}_8$  [17,18] and  $\text{LiCoMnO}_4$  [24] showed a long plateau over 4.5 V, Tables 1 and 2.

The initial discharge profile of a cell with  $\text{LiCoMnO}_4$  [24] as the cathode has capacity of ca. 95 mA h  $\text{g}^{-1}$  at the long plateau centered on 5.0 V, Fig. 3, and therefore energy density of ca. 475 W h  $\text{kg}^{-1}$ . This is higher than ca. 456 W h  $\text{kg}^{-1}$  (ca. 120 mA h  $\text{g}^{-1}$  at 3.8 V) [42] obtained with  $\text{LiMn}_2\text{O}_4$ , and approaches ca. 518 W h  $\text{kg}^{-1}$  (ca. 140 mA h  $\text{g}^{-1}$  at 3.7 V) [42] attained with  $\text{LiCoO}_2$ . A new cathode material,  $\text{Li}_{1.5}\text{Na}_{0.5}\text{MnO}_{2.85}\text{I}_{0.12}$ , had similar energy density to  $\text{LiCoMnO}_4$ , ca. 468 W h  $\text{kg}^{-1}$  (ca. 180 mA h  $\text{g}^{-1}$  at 2.6 V), at a current density of 0.5 mA  $\text{cm}^{-2}$  [14].  $\text{LiCoMnO}_4$ , however, exhibits almost double the mid-discharge voltage of  $\text{Li}_{1.5}\text{Na}_{0.5}\text{MnO}_{2.85}\text{I}_{0.12}$ , and thus has distinct features as a cathode material. The plateau centered on 5.0 V exhibits good cycling stability, maintaining its discharge capacity to well over 35 cycles [24]. The high energy density and the good cyclability attained render  $\text{LiCoMnO}_4$  potentially very attractive as a cathode material in large scale Li ion batteries, toward realizing ZEV.

## Acknowledgements

HK thanks CVCP for an ORS Award.

## References

- [1] B. Scrosati, *Nature* 373 (1995) 557.
- [2] K. Brandt, *Solid State Ionics* 69 (1994) 173.
- [3] R. Koksabang, J. Barker, H. Shi, M.Y. Saidi, *Solid State Ionics* 84 (1996) 1.
- [4] P.G. Bruce, *Chem. Commun.* (1997) 1817.
- [5] K. Mizushima, P.C. Jones, P.C. Wiseman, J.B. Goodenough, *Mater. Res. Bull.* 15 (1980) 783.
- [6] T. Nagaura, K. Tozawa, *Prog. Batteries Sol. Cells* 9 (1990) 209.
- [7] T. Ohzuku, M. Kitagawa, T. Hirai, *J. Electrochem. Soc.* 137 (1990) 769.
- [8] J.-M. Tarascon, E. Wang, F.K. Shokoohi, W.R. McKinnon, S. Colson, *J. Electrochem. Soc.* 138 (1991) 2859.
- [9] A. Yamada, K. Miura, K. Hinokuma, M. Tanaka, *J. Electrochem. Soc.* 142 (1995) 2149.
- [10] Japan Electronics, March 6, 1996.
- [11] JEC Battery Newsletter, Sony Battery Group and Sony Energytec, July–August (1993) 19.
- [12] A.R. Armstrong, P.G. Bruce, *Nature* 381 (1996) 499.
- [13] P.G. Bruce, A.R. Armstrong, H. Huang, *J. Power Sources* 68 (1997) 19.
- [14] J. Kim, A. Manthiram, *Nature* 390 (1997) 265.
- [15] J.-M. Tarascon, D. Guyomard, *Solid State Ionics* 69 (1994) 293.
- [16] D. Guyomard, J.-M. Tarascon, *J. Power Sources* 54 (1995) 92.
- [17] Q. Zhong, A. Bonakdarpour, M. Zhang, Y. Gao, J.R. Dahn, *J. Electrochem. Soc.* 144 (1997) 205.
- [18] K. Amine, H. Tukamoto, H. Yasuda, Y. Fujita, *J. Power Sources* 68 (1997) 604.
- [19] G.T.-K. Fey, W. Li, J.R. Dahn, *J. Electrochem. Soc.* 141 (1994) 2279.
- [20] C. Sigala, D. Guyomard, A. Verbaere, Y. Piffard, M. Tournoux, *Solid State Ionics* 81 (1995) 167.
- [21] Y. Ein-Eli, W.F. Howard Jr., *J. Electrochem. Soc.* 144 (1997) L205.
- [22] Y. Ein-Eli, W.F. Howard Jr., S.H. Lu, S. Mukerjee, J. McBreen, J.T. Vaughan, M.M. Thackeray, *J. Electrochem. Soc.* 145 (1998) 1238.
- [23] H. Kawai, M. Nagata, H. Tukamoto, A.R. West, *J. Mater. Chem.* 8 (1998) 837.
- [24] H. Kawai, M. Nagata, H. Tukamoto, A.R. West, *J. Electrochem. Soc.* (1998), submitted.
- [25] H. Kawai, M. Nagata, M. Tabuchi, H. Tukamoto, A.R. West, *Chem. Mater.* (1998), submitted.
- [26] G. Blasse, *Philips Res. Rep. Suppl.* 3 (1964) 1.
- [27] V.S. Hernandez, L.M.T. Martinez, G.C. Mather, A.R. West, *J. Mater. Chem.* 6 (1996) 1533.
- [28] H. Kawai, M. Tabuchi, M. Nagata, H. Tukamoto, A.R. West, *J. Mater. Chem.* 8 (1998) 1273.
- [29] M.A. Lafontaine, M. Leblanc, G. Ferey, *Acta Crystallogr. C* 45 (1989) 1205.
- [30] S.J. Marin, M. O’Keeffe, D.E. Partin, *J. Solid State Chem.* 113 (1994) 413.
- [31] S. Suzuki, M. Tomita, S. Okada, H. Arai, *J. Phys. Chem. Solids* 57 (1996) 1851.
- [32] K. Amine, H. Tukamoto, H. Yasuda, Y. Fujita, *J. Electrochem. Soc.* 143 (1996) 1607.
- [33] S.R.S. Prabaharan, M.S. Michael, S. Radhakrishna, C. Julien, *J. Mater. Chem.* 7 (1997) 1791.
- [34] F. Orsini, E. Baudrin, S. Denis, L. Dupont, M. Touboul, D. Guyomard, Y. Piffard, J.-M. Tarascon, *Solid State Ionics* 107 (1998) 123.
- [35] C. Sigala, A. Verbaere, J.L. Mansot, D. Guyomard, Y. Piffard, M. Tournoux, *J. Solid State Chem.* 132 (1997) 372.
- [36] S. Kano, M. Sato, *Solid State Ionics* 79 (1995) 215.
- [37] G.T.-K. Fey, J.R. Dahn, M. Zhang, W. Li, *J. Power Sources* 68 (1997) 549.
- [38] H. Kageyama, H. Kawai, A.R. West, unpublished data.
- [39] C. Gonzalez, M. Gaitan, M.L. Lopez, M.L. Veiga, R. Saez-Puche, C. Pico, *J. Mater. Sci.* 29 (1994) 3458.
- [40] Y. Gao, K. Myrtle, M. Zhang, J. Reimers, J.R. Dahn, *Phys. Rev. B* 54 (1996) 16670.
- [41] T. Zheng, J.R. Dahn, *Phys. Rev. B* 56 (1997) 3800.
- [42] D. Linden (Ed.), *Handbook of Batteries*, 2nd edn., 36, 10, McGraw-Hill, New York, 1995.
- [43] G. Ceder, Y.-M. Chiang, D.R. Sadoway, M.K. Aydinol, Y.-I. Jang, B. Huang, *Nature* 392 (1998) 694.
- [44] M.K. Aydinol, A.F. Kohan, G. Ceder, K. Cho, J. Joannopoulos, *Phys. Rev. B* 56 (1997) 1354.
- [45] E.J.W. Verwey, P.B. Braun, E.W. Gorter, F.C. Romeijn, J.H. van Santen, *Z. Phys. Chem.* 198 (1951) 6.
- [46] E.G. Larson, R.J. Arnott, D.G. Wickham, *J. Phys. Chem. Solids* 23 (1962) 1771.
- [47] S.E. Dorris, T.O. Mason, *J. Am. Ceram. Soc.* 71 (1988) 379.
- [48] V. Massarotti, D. Capsoni, M. Bini, G. Chiodelli, C.B. Azzoni, M.C. Mozzati, A. Paleari, *J. Solid State Chem.* 131 (1997) 94.